

GT2011-458&

## ROTOR DYNAMIC EVALUATION OF CENTRIFUGAL COMPRESSOR USING ELECTROMAGNETIC EXCITER

### Naohiko Takahashi

Tsuchiura Research Laboratory  
Research & Development Group  
Hitachi Plant Technologies, Ltd.  
Tsuchiura-shi, Ibaraki, Japan

### Yohei Magara

Mechanical Engineering Research Laboratory  
Hitachi, Ltd.  
Hitachinaka-shi, Ibaraki, Japan

### Mitsuhiro Narita

Compressor Division  
Hitachi Plant Technologies, Ltd.  
Tsuchiura-shi, Ibaraki, Japan

### Haruo Miura

Tsuchiura Research Laboratory  
Research & Development Group  
Hitachi Plant Technologies, Ltd.  
Tsuchiura-shi, Ibaraki, Japan

### ABSTRACT

Since heavier gases exert larger effects on rotordynamic stability, stability evaluation is important in developing or designing high-pressure compressors. To evaluate the rotor stability during operation, an excitation test using a magnetic bearing is the most practical method. In stability analysis, labyrinth seals can produce significant cross-coupling forces, which particularly reduce the damping ratio of the first forward mode. Therefore, forward modes should be distinguished from backward modes in the excitation test. One method that excites only the forward modes, not the backward modes (and vice versa), is the use of a rotating excitation. In this method, the force is simultaneously applied to two axes to excite the rotor in circular orbits. Two trigonometric functions, i.e., cosine and sine functions, are used to generate this rotation force. Another method is the use of a unidirectional excitation and a mathematical operation to distinguish the forward whirl from the backward whirl. In this method, a directional frequency response function that separates the two modes in the frequency domain is obtained from four frequency response functions by using a complex number expression for the rotor motion. In this study, the latter method was employed to evaluate the rotor stability of a high-pressure compressor. To obtain the frequencies and damping ratios of the eigenvalues, the curve fitting based on system identification methods, such as the prediction error method, was introduced for the derived frequency response functions. Firstly, these methods were applied to a base evaluation under a low-pressure gas operation,

in which the stability mainly depends on the bearing property. Using the obtained results, the bearing coefficients were estimated. Next, the same methods were applied to stability evaluations under high-pressure gas operations. The destabilizing forces were also estimated from the test results and compared with the calculation results.

### NOMENCLATURE

$c$	damping coefficient
$c_{xx}$	$x$ -axis damping coefficient
$c_{yy}$	$y$ -axis damping coefficient
dFRF	directional frequency response function
$f_n$	natural frequency
$f_r$	complex number representation of magnetic force
FRF	frequency response function
$f_x$	$x$ -axis magnetic force
$f_y$	$y$ -axis magnetic force
$k_{xx}$	$x$ -axis stiffness coefficient
$k_{yy}$	$y$ -axis stiffness coefficient
$k$	stiffness coefficient
$G_p$	compliance of rotor system
MIMO	multi-input and multi-output
PEM	prediction error method
$q$	cross-coupled stiffness coefficient
$Q_A$	total cross-coupled stiffness coefficient by API Level 1
$r$	complex number representation of displacement
SISO	single-input and single-output
$x$	$x$ -axis rotor displacement

$y$   $y$ -axis rotor displacement  
 $\delta$  logarithmic decrement  
 $\omega_i$  angular natural frequency

## INTRODUCTION

Recently, many projects regarding carbon dioxide capture and storage (CCS) or enhanced oil recovery (EOR) have been implemented and the demands of high-pressure injection compressors increase. In such high-pressure compressors, the high-density gas affects rotor stability; thus, evaluating the rotor stability is one of the most important tasks in designing the high-pressure compressors. This stability problem, however, is not new. The requirements and procedures of stability analysis are already described in American Petroleum Institute (API) Standard 617, Seventh Edition (2002) [1].

For a compressor system, the rotor stability mainly relies on bearings and seals. In the rotordynamic analysis, the bearings and seals are modeled and their dynamic effects are included in the rotor-bearing system. To verify the accuracy of the bearing and seal models, the measurement of these dynamic properties has been carried out by using special test rigs [2]. By applying empirically supported techniques, the rotor stability is confirmed during the design stage, but it is still desired to measure the actual stability during full pressure and full load tests. There are some reports that describe stability measurements, in which a magnetic bearing exciter was installed at the shaft end and logarithmic decrements were identified [3-6].

There are several indices that represent the stability of a rotor vibration. In API Standard 617, the logarithmic decrement of the first forward damped mode is used as an index for rotor stability evaluation. During rotation, the vibration modes split into the forward and backward modes owing to the gyroscopic effect of rotational disks and/or cross-coupled stiffness induced in seals and/or bearings. As rotational speed increases, the swirling fluid in seal gaps leads to cross-coupled stiffness growth, which reduces the damping of the forward mode. Therefore, the logarithmic decrement of the forward mode should be identified to evaluate the rotor stability.

For measuring the rotor stability during operation, an excitation test using a magnetic bearing is the most practical method. The stability evaluation could be carried out done in the frequency or time domain. Pettinato et al. identified the logarithmic decrements of the forward and backward modes of a compressor using multiple output backward autoregression, which is one of the time domain techniques [6]. In the frequency domain, frequency-sweep excitation is most commonly used. The logarithmic decrements can be identified from the derived frequency response function (FRF), but much effort is required in the identification. A radial magnetic bearing has two control axes ( $x$ - and  $y$ -axes) that are mutually orthogonal and also orthogonal to the rotating axis. In a single-input and single-output (SISO) measurement, the derived FRF shows a heavy overlapping of the forward and backward

modes. There are several methods that can be used to prevent this overlapping. One method is the use of a bidirectional rotating excitation. In this method, two synchronized unidirectional trigonometric forces are used. If the phase difference of these forces is 90 degrees, a circular forward or backward rotating excitation is formed. To obtain FRFs, shaft responses are simultaneously measured during excitation. For this method, however, a special device that generates bidirectional rotating forces is required. Another method is the use of a unidirectional excitation, which does not require a special instrument and can be performed using a commercially available instrument. In this method, a multi-input and multi-output (MIMO) measurement is performed, consequently obtaining four relations between two inputs and two outputs for one local exciter. To identify the forward and backward mode eigenvalues from these input-output relations, system identification techniques for the MIMO system can be applied.

This paper deals with a high-pressure gas compressor and focuses on its stability evaluation based on the latter method that uses a unidirectional excitation. In system identification, the MIMO system techniques are applied to the sets of FRFs measured during operation. The measured FRFs are also transformed to a directional frequency response function (dFRF) by introducing complex numbers [7, 8]. In a dFRF, the forward and backward modes are distinguished by the direction of the frequency axis. The eigenvalues are identified by applying system identification techniques to the sets of FRFs and/or dFRFs. The stability test consists of three steps. In the first step, the test was conducted under a low gas pressure. The bearing property can be evaluated using the results of this test step. In the next two steps, the tests were conducted under high gas pressures. Two types of gases, nitrogen ( $N_2$ ) and carbon dioxide ( $CO_2$ ), were used and load tests were carried out. For each condition, the rotor stability was evaluated. The damping and cross-coupled stiffness of seals were analyzed using the identified eigenvalues.

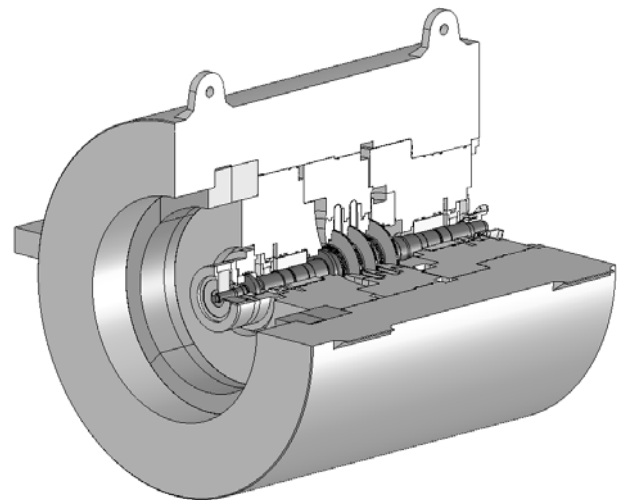


**Figure 1: Tested high-pressure compressor**

## HIGH-PRESSURE COMPRESSOR

Figure 1 shows the high-pressure centrifugal compressor for stability evaluation. The compressor has three stages in a straight-through configuration. In the aerodynamic design, a pure CO<sub>2</sub> gas is planned to be used as the test gas. The rated compressor power is 1,935 kW at the design operating speed of 14,100 min<sup>-1</sup> and the maximum continuous speed is 14,805 min<sup>-1</sup>. The rotor weights 167 kg and has a bearing span of 1063 mm. The rotor is supported on five-shoe tilt pad journal bearings with a rocker pivot in the load on the pad configuration. The bearings have a 90 mm diameter and an L/D ratio of 0.422. The balance piston seal is of the three-step labyrinth type without shunts or swirl brakes that generate a high damping. Impeller-eye seals are of the stepped labyrinth type also without antistirl devices. Dry gas seals are employed at end seal locations. The suction and discharge pressures at the design point are 6.08 MPa (abs) and 19.6 MPa (abs), respectively, and the discharge gas density is 270.5 kg/m<sup>3</sup>. The casing design pressure is 50 MPa, which is much higher than the operation pressure. This high pressure was aimed at confirming the design and manufacturing processes.

Figure 2 provides a plot of critical speed ratio (CSR) versus gas density, which is used as one of the criteria for API Level I screening. The design position of the subject compressor is located in region B, which is a higher risk region where API Level II stability analysis is typically required.

Figure 3 shows the compressor on the test stand. The compressor is driven by an induction motor via an increasing speed gear. To change the running speed, a variable frequency drive is used.

One of the objectives of the test using this compressor is to evaluate the rotor stability during high-pressure operations. To measure the frequency and damping ratio of the eigenvalues, the rotor is required to be excited asynchronously. For this purpose, an electromagnetic exciter was attached to the shaft end of the suction side (nondrive end). Figure 4 shows the details of the exciter. The exciter has the same configuration as a heteropolar radial magnetic bearing. The inner diameter of the electromagnet stator is 70 mm. The magnetic force produced by the magnets is 888 N at maximum currents. An asynchronously oscillating force produced by the magnets is injected into the rotor to excite the eigen modes. The eddy current sensors facing the end of the shaft detect the rotor displacements of radial directions. The shaft response is measured while sweeping the frequency of the exciting force, so that transfer functions can be determined. There are two control axes (*x*- and *y*-axes) in the exciter, which are also defined as the coordinate axes that express the rotor motion. The compressor shaft rotates from the *x*-axis to the *y*-axis, which is defined as the positive rotation direction.

## PARAMETRIC IDENTIFICATION METHODS

A popular method used to identify the damping factor of the vibration system is the so-called half-power method. Even though the half-power method is easy to use, there is difficulty

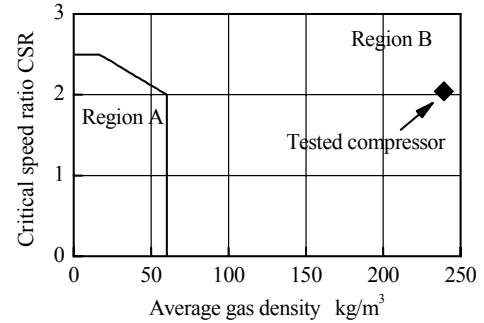


Figure 2: API617 Level I screening criteria



Figure 3: Photo of compressor in test facility

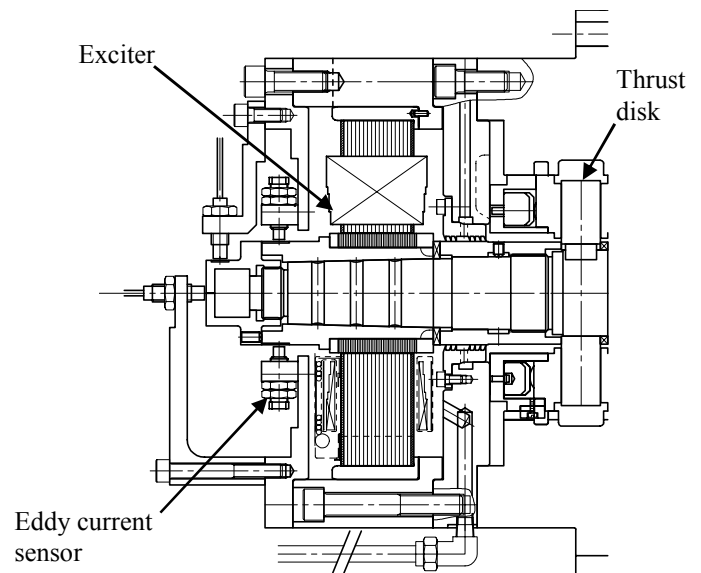


Figure 4: Compressor shaft end with exciter

in evaluating a highly damped case. In the system identification field, parametric identification methods are widely used for the parameter estimation of a given model

structure. Some of these methods, e.g., a prediction error method (PEM), lead to better estimation results and can be applied to the MIMO system.

Now, a sample comparison of identification results is provided. As reference results for the comparison, frequency response and eigenvalue analyses were carried out by a finite element method (FEM) for the high-pressure compressor rotor under a certain bearing support condition. The half-power method and the parametric identification by the PEM were applied to the FRF obtained by FEM analysis. Table 1 shows the identified eigenvalues for accuracy comparison. The PEM shows good agreement with the reference derived by FEM analysis. In this identification method, MATLAB<sup>1</sup> was used. The half-power method, however, shows poor agreement with the reference damping.

### SYSTEM IDENTIFICATION FOR ROTOR SYSTEM

To identify the forward and backward modes of the rotating system separately, the system identification techniques for the MIMO system are required. The PEM is one of those techniques that can handle a MIMO system. When using a unidirectional excitation, the forward and backward mode responses overlap. If the PEM is used, this overlapping is prevented in the eigenvalue identification. The PEM, however, directly treats the FRFs in the estimation process; thus, the forward and backward mode responses are not presented explicitly in the estimated responses. In the next paragraph, a matrix transforming process for obtaining dFRFs from the set of unidirectional FRFs will be presented. In the dFRFs, the forward and backward responses separately appear in the frequency domains of positive and negative axes.

In general, the relationship between the excitation force and the displacement of the rotor is expressed in the transfer function form as

$$\begin{bmatrix} x \\ y \end{bmatrix} = \begin{bmatrix} G_{p_{xx}} & G_{p_{xy}} \\ G_{p_{yx}} & G_{p_{yy}} \end{bmatrix} \begin{bmatrix} f_x \\ f_y \end{bmatrix}, \quad (1)$$

where  $G_{p_{ij}}$  ( $i, j=x, y$ ) is the compliance of the rotor system. To express the forward and backward whirls, complex numbers are introduced by

$$\begin{aligned} r &= x + iy, & \tilde{f}_r &= f_x + if_y, \\ \bar{r} &= x - iy, & \tilde{f}_{\bar{r}} &= f_x - if_y. \end{aligned} \quad (2)$$

Substituting Eqn.(2) into Eqn.(1), the following relation is obtained

$$\begin{bmatrix} r \\ \bar{r} \end{bmatrix} = \begin{bmatrix} G_{p_{rr}} & G_{p_{r\bar{r}}} \\ G_{p_{\bar{r}r}} & G_{p_{\bar{r}\bar{r}}} \end{bmatrix} \begin{bmatrix} \tilde{f}_r \\ \tilde{f}_{\bar{r}} \end{bmatrix}, \quad (3)$$

**Table 1 Comparison of identification methods**

	Frequency Hz (Error)	Damping ratio (Error)
Exact solution by FEM	124.4	0.03260
Estimated by PEM	124.5 (0.08 %)	0.03253 (-0.21 %)
Estimated by half-power method	123.22 (-0.95 %)	0.04295 (31.7 %)

$$G_{p_{rr}} = \frac{1}{2} \{ G_{p_{xx}} + G_{p_{yy}} + i(G_{p_{yx}} - G_{p_{xy}}) \},$$

$$G_{p_{r\bar{r}}} = \frac{1}{2} \{ G_{p_{xx}} - G_{p_{yy}} + i(G_{p_{yx}} + G_{p_{xy}}) \},$$

$$G_{p_{\bar{r}r}} = \frac{1}{2} \{ G_{p_{xx}} - G_{p_{yy}} - i(G_{p_{yx}} + G_{p_{xy}}) \},$$

$$G_{p_{\bar{r}\bar{r}}} = \frac{1}{2} \{ G_{p_{xx}} + G_{p_{yy}} - i(G_{p_{yx}} - G_{p_{xy}}) \}.$$

In Eqn.(3), the upper diagonal element provides the directional frequency response function, in which the forward and backward modes are separated in the frequency axis. In the above equations, the following holds:

$$G_{p_{jk}}(-i\omega) = \overline{G_{p_{jk}}(i\omega)}, \quad j, k = x, y. \quad (4)$$

The FRFs in the negative frequency region can be obtained from the above equations.

### EXPERIMENTAL RESULTS OF IDENTIFICATION

This section presents some results of system identification for the experiments. In the experiments, N<sub>2</sub> gas was used and the suction pressure was kept at 6.24 MPa (abs). The rotational speed was set at 14100 min<sup>-1</sup>, and then the discharge pressure became 10.8 MPa (abs). The set of FRFs presented in Eqn.(1) was measured by swept unidirectional excitations. For the measured data, two methods of system identification were applied. The first method uses a MIMO system identification technique with the PEM. The second method uses a SISO system identification technique with the PEM also, but the set of FRFs is transformed to a dFRF before applying the PEM.

Figure 5 shows the bode diagrams of the set of measured FRFs. In these diagrams, the first and second modes are included in the frequency domain. The disturbance at 235 Hz is due to the unbalance vibration. Figures concerning  $G_{p_{yx}}$  and  $G_{p_{yy}}$  are not shown, because they are similar to those concerning  $G_{p_{xy}}$  and  $G_{p_{xx}}$ .

Figure 6 shows the curve fitting results obtained by the first method, i.e., MIMO FRF identification for the first mode. This indicates that all the curves were fitted simultaneously. Figure 7 shows the dFRF transformed from the set of FRFs. In Figure 5, the existence of the forward and backward modes is

<sup>1</sup> MATLAB is a registered trademark of The MathWorks, Inc.

observed, particularly in the second mode, but the frequency and damping of the forward and backward modes are hardly distinguished. After transforming to the dFRF, the forward and backward modes are clearly separated in the bode diagrams. In these diagrams, the forward modes appear in the positive frequency domain of  $G_{pr}$  and the backward modes appear in the negative frequency domain of  $G_{pr}$ . This reveals that the stability of the first forward mode is lower than that of the first backward mode. This is due to the fact that cross-coupled stiffness that destabilizes the forward modes and stabilizes the backward modes is produced in the seals and/or impellers. This also reveals that the resonant frequency of the second forward mode is higher than that of the second backward mode. This frequency shift was mainly caused by a gyroscopic effect. For the positive and negative frequency domains of the dFRF, the PEM was applied individually in accordance with the SISO system identification method. Figure 8 shows the curve fitting results derived by this identification method. It can be seen that the identification result derived from the dFRF is better than that derived from the MIMO FRF, in which a small discrepancy between the identified model and the measurements remains. In unidirectional excitations, nondiagonal elements, i.e.,  $G_{px}$  and  $G_{py}$ , often have a low signal-to-noise ratio owing to the small gyroscopic effect or cross-coupled stiffness of seals. This leads to a poor curve fitting result in the MIMO FRF

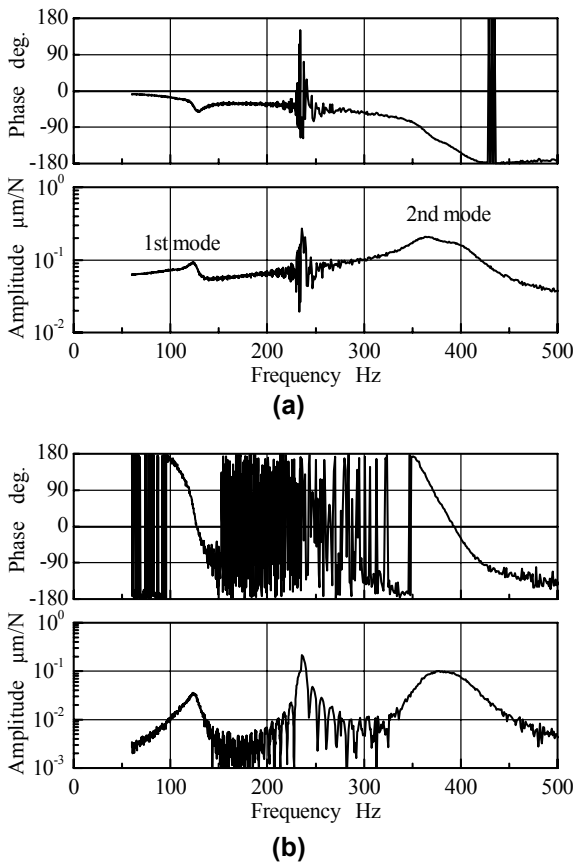


Figure 5: Measured FRFs: (a)  $G_{p_{xx}}$  and (b)  $G_{p_{xy}}$

identification method. When using the SISO dFRF identification method, the noise in the nondiagonal elements is merged into the diagonal elements; thus, the SISO dFRF identification method provides better results than the MIMO FRF identification method.

Table 2 shows the frequencies and damping factors of the eigenvalues derived by the MIMO FRF and SISO dFRF identification methods. In this experiment, anisotropies in the bearings and seals were small; thus, the SISO dFRF identification method was better suited. However, in the case of the rotor system with large anisotropies, the MIMO FRF or MIMO dFRF identification method is a better choice. In the following sections, the SISO dFRF identification method is basically applied to evaluate the rotor stability.

### BASE STABILITY EVALUATION

To obtain the stability free from gas forces in seals, a low-gas-pressure test was performed. When the seal forces are small, the eigenvalues are mainly determined by the stiffness and damping of the bearing support. Figure 9 shows the results of eigenvalue identifications under a low-gas-pressure operating condition and different rotational speeds. During these measurements, the suction pressure of the compressor was kept at 0.2 MPa (abs). The bearing pad preload and clearance ratio were adjusted to be 0.29 and 0.0018, respectively. The

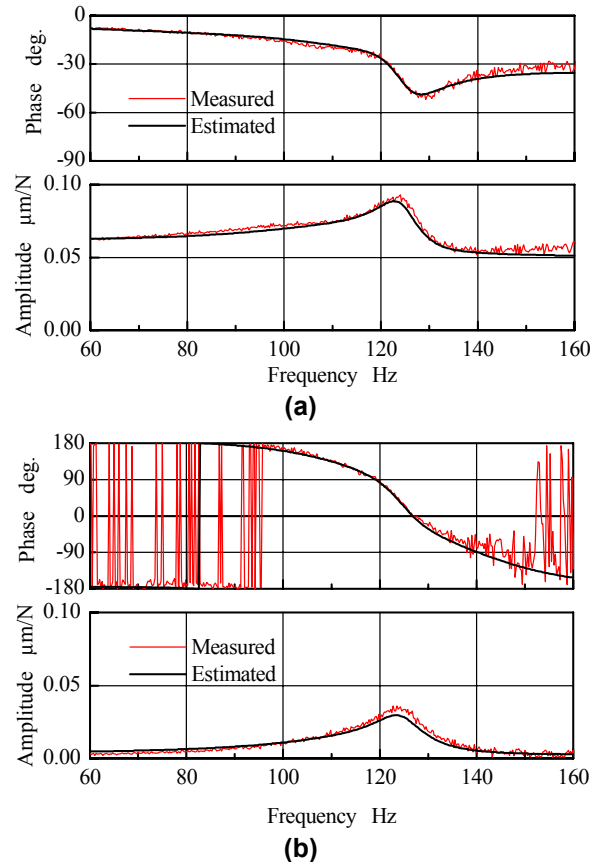
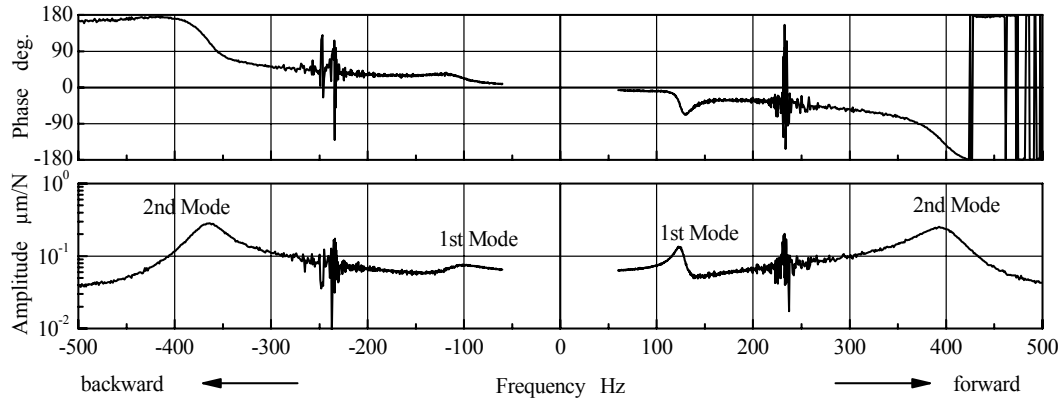
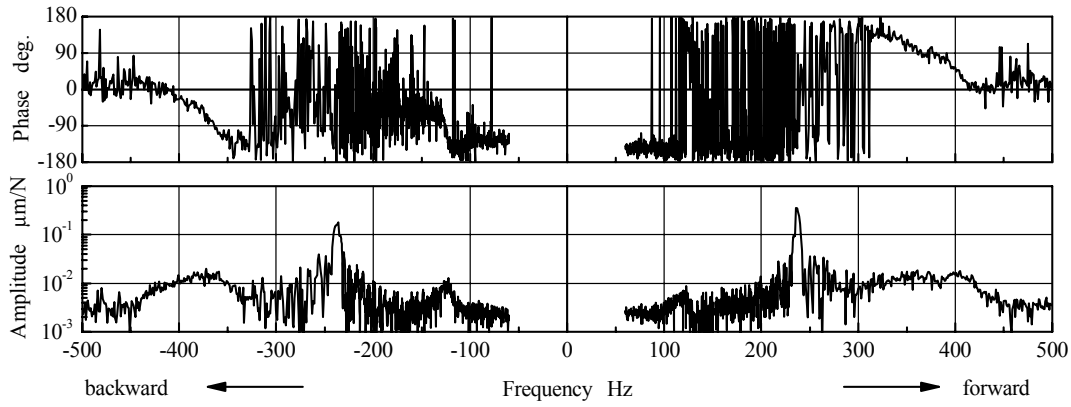


Figure 6: MIMO curve fit model versus measured FRFs: (a)  $G_{p_{xx}}$  and (b)  $G_{p_{xy}}$

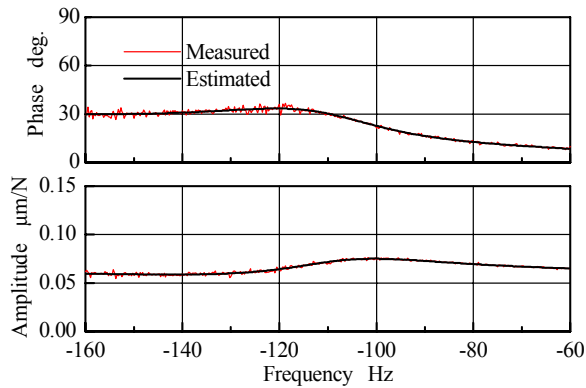


(a)

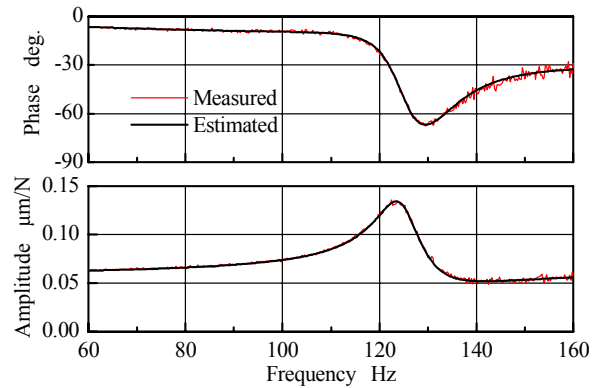


(b)

Figure 7: dFRF transformed from FRFs: (a)  $G_{pr\bar{r}}$  and (b)  $G_{pr\bar{i}}$



(a)



(b)

Figure 8: Curve fit model versus measured dFRF,  $G_{pr\bar{r}}$  : (a) backward and (b) forward parts

bearing oil type used was ISO VG46, and the inlet oil temperature was kept at 45 °C.

The eigenvalues can also be calculated by using the finite element (FE) model that includes the calculated bearing coefficients. If the model error of the rotor itself is small, the calculation error of eigenvalues originates from the bearing coefficients. In this study, the bearing coefficients were estimated by iterative correction so that the calculated

eigenvalues coincided with the measured ones. Figure 10 shows the estimated bearing coefficients, i.e., direct stiffness  $k$  and direct damping  $c$ . Before estimating these coefficients, the rotor FE model was reconciled by modal testing to improve its accuracy. For the iterative correction in the estimation process, the two bearings were assumed as identical and isotropic, and a simplex method for function minimization in MATLAB was used. Although not shown, the bearing

**Table 2 Comparison of MIMO FRF and SISO dFRF identification methods**

	Frequency Hz	Damping ratio
MIMO FRF	124.6	0.0412
	113.7	0.2003
SISO dFRF	124.9	0.0397
	110.1	0.1810

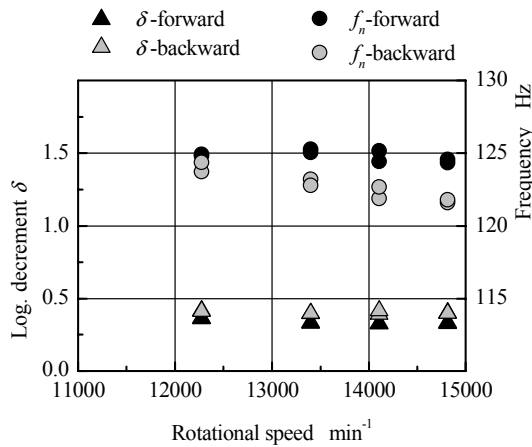


**Figure 9: Eigenvalues identified under base condition**

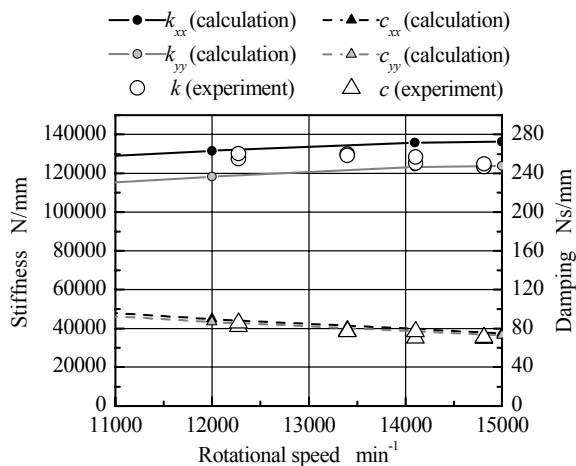


**Figure 10: Estimated bearing coefficients**

coefficients in the cross-coupling term were also estimated. The bearing coefficients calculated using in-house software are also plotted in Figure 10. In the bearing calculation, a full-coefficient-based model was used and the obtained full coefficients were reduced to eight nonsynchronous coefficients at the first natural frequency of the rotor. The results confirmed that the calculation model has good accuracy.

**LOAD TEST RESULTS**

For load tests, N<sub>2</sub> and CO<sub>2</sub> gases were used and stability evaluations were conducted for each gas operation. The

suction pressure was kept at 6 MPa (abs) and excitation tests were conducted at several rotational speeds. The flow rate was adjusted at the design point for each speed. Figure 11 shows the identified logarithmic decrements of the first forward mode under each test condition. As stated previously, the high-pressure gases reduce the damping of the first forward mode, because the tested compressor has no antiswirl device at the seals. The stability of the CO<sub>2</sub> gas operation is worse than that of the N<sub>2</sub> gas operation. This is because a heavier gas and a larger differential pressure at the balance piston seal produce a larger cross-coupled stiffness.

In API Standard 617, the modified Alford’s method is employed for Level I stability analysis. In this study, the API cross-coupled stiffness was determined by using the same procedure for the inverse estimation of the bearing coefficients. In this estimation procedure for the high-pressure gas effects, the experimental bearing coefficients indicated in the previous section were used as the bearing model. Eigenvalue calculations were performed with a set of coefficients introduced at the rotor midspan between bearings, and the coefficients were estimated by iterative correction so that the calculated eigenvalues coincided with the measured ones. Figure 12 shows the estimated cross-coupled stiffness  $q$  and damping  $c\omega_1$  of the N<sub>2</sub> gas effects, where  $\omega_1$  is the angular frequency of the first forward mode. In this figure, the damping term is not small, but the cross-coupled stiffness term is larger than the damping term. The difference between the cross-coupled stiffness and damping terms destabilizes the rotor system. Figure 13 shows the amount of difference and the anticipated cross-coupled stiffness  $Q_A$  calculated using the API-modified Alford’s equation. For this specific compressor, the API equation yields almost half of the destabilizing effect derived by experiments. For CO<sub>2</sub> gas effects, the estimation of the coefficients was not successful because of overdamped backward eigenvalues.

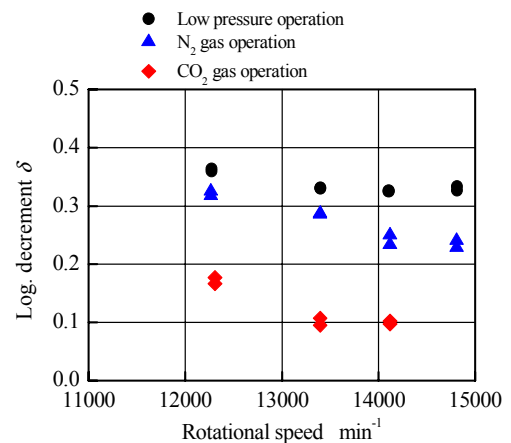


**Figure 11: Identified logarithmic decrements of first forward mode**

## CONCLUSIONS

Stability evaluation methods that use unidirectional exciting forces were demonstrated. Parametric system identification methods are powerful tools for identifying the eigenvalues of rotor systems. In this study, prediction error methods were used and provided good accuracy. To identify the eigenvalues of the forward and backward modes separately, MIMO FRF and SISO dFRF identification methods were employed. In the dFRF identification method, the separation of the forward and backward responses in the frequency domain was demonstrated. A base stability test and high-pressure gas tests were carried out. Using the test results, the bearing coefficients and the API cross-coupled stiffness were

estimated inversely. A comparison of the estimated and calculated coefficients shows modest agreement.

## REFERENCES

- [1] API, 2002, "Axial and Centrifugal Compressors and Expander-compressors for Petroleum, Chemical and Gas Industry Services", STD 617 Seventh Edition, American Petroleum Institute
- [2] Wagner, N. G., Steff, K., 1996, "Dynamic Labyrinth Coefficients from a High-Pressure Full-Scale Test Rig Using Magnetic Bearings, Rotordynamic Instability Problems in High-Performance Turbomachinery", NASA-CP-3344, Texas, pp. 95–111.
- [3] Moore, J. J., Walker, S. T., Kuzszal, M. J., 2002, "Rotordynamic Stability Measurement During Full-Load, Full-Pressure Testing of a 6000 PSI Reinjection Centrifugal Compressor", Proc. of 31th Turbomachinery Symposium, Texas, pp. 29–38.
- [4] Sorokes, J. M., Soulas, T. A., Koch, J. M., Gilarranz R, J. L., 2009, "Full-Scale Aerodynamic and Rotordynamic Testing for Large Centrifugal Compressors", Proc. of 38th Turbomachinery Symposium, Texas, pp. 71–79.
- [5] Bidaut, Y., Baumann, U., Al-Harthy, S. M. H., 2009, "Rotordynamic Stability of a 9500 PSI Reinjection Centrifugal Compressor Equipped with Hole Pattern Seal – Measurement Versus Prediction Taking into Account the Operational Boundary Conditions", Proc. of 38th Turbomachinery Symposium, Texas, pp. 251–259.
- [6] Pettinato, B. C., Cloud, C. H., Campos, R. S., 2010, "Shop Acceptance Testing of Compressor Rotordynamic Stability and Theoretical Correlation", Proc. of 39th Turbomachinery Symposium, Texas, pp. 31–42.
- [7] Lee, C. W., 1991, "A Complex Modal Testing Theory for Rotating Machinery", Mechanical System and Signal Processing, **5**, pp. 119–137
- [8] Takahashi, N., Fujiwara, H., Matsushita, O., Ito, M., Fukushima, Y., 2007, "An Evaluation of Stability Indices Using Sensitivity Function for Active Magnetic Bearing Supported High-Speed Rotor", ASME, Journal of Vibration and Acoustics, **129**, pp. 230–238

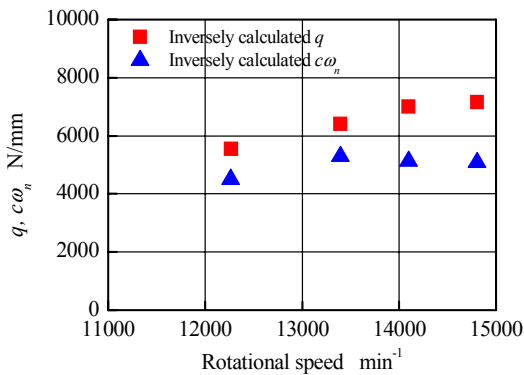


Figure 12: Estimated coefficients of gas effects

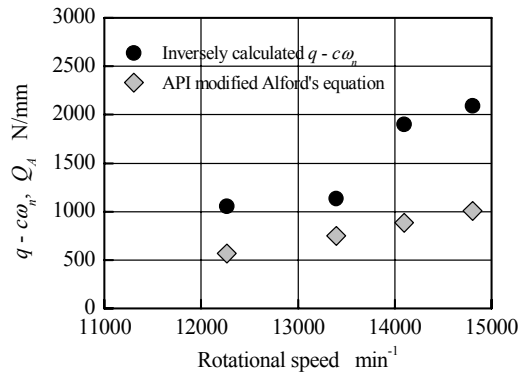


Figure 13: Comparison of estimated coefficients and API cross-coupled stiffness